© 2018. Published by The Company of Biologists Ltd | Development (2018) 145, dev168906. doi:10.1242/dev.168906

TECHNIQUES AND RESOURCES

RESEARCH ARTICLE

Simultaneous zygotic inactivation of multiple genes in mouse through CRISPR/Cas9-mediated base editing

He Zhang[1,2,*], Hong Pan[1,3,*], Changyang Zhou[1,2,*], Yu Wei[1], Wenqin Ying[1], Shuting Li[1], Guangqin Wang[1], Chao Li[1], Yifei Ren[1,2], Gen Li[4,5,6], Xu Ding[4,5,6], Yidi Sun[2,8], Geng-Lin Li[4,5,6,7], Lei Song[4,5,6], Yixue Li[2,8,9,10], Hui Yang[1,‡] and Zhiyong Liu[1,‡]

ABSTRACT

In vivo genetic mutation has become a powerful tool for dissecting gene function; however, multi-gene interaction and the compensatory mechanisms involved can make findings from single mutations, at best difficult to interpret, and, at worst, misleading. Hence, it is necessary to establish an efficient way to disrupt multiple genes simultaneously. CRISPR/Cas9-mediated base editing disrupts gene function by converting a protein-coding sequence into a stop codon; this is referred to as CRISPR-stop. Its application in generating zygotic mutations has not been well explored yet. Here, we first performed a proof-of-principle test by disrupting *Atoh1*, a gene crucial for auditory hair cell generation. Next, we individually mutated *vGlut3* (*Slc17a8*), otoferlin (*Otof*) and prestin (*Slc26a5*), three genes needed for normal hearing function. Finally, we successfully disrupted *vGlut3*, *Otof* and prestin simultaneously. Our results show that CRISPR-stop can efficiently generate single or triple homozygous F0 mouse mutants, bypassing laborious mouse breeding. We believe that CRISPR-stop is a powerful method that will pave the way for high-throughput screening of mouse developmental and functional genes, matching the efficiency of methods available for model organisms such as *Drosophila*.

KEY WORDS: Inner ear, vGlut3, Prestin, Otoferlin, Base editing, CRISPR/Cas9

INTRODUCTION

The clustered regularly interspaced short palindromic repeat (CRISPR) system has been developed as a versatile genome editing tool in various organisms (Cong et al., 2013; Yao et al., 2018; Zhou et al., 2018). The Cas9 protein, guided by small guide RNA (sgRNA), binds to its target DNA site on the genome and works as a nuclease to induce double-stranded breaks (DSBs) (Zuo et al., 2017). The traditional CRISPR/Cas9 gene targeting approach inevitably introduces random insertions and deletions (indels) that cannot be controlled, and the double-stranded DNA cleavage by wild-type Cas9 has been shown to result in excessive DNA damage and cell death (Hart et al., 2015; Wang et al., 2015). Recently, Cas9 nickase (nCas9) has been fused with cytidine deaminase (APOBEC1) and uracil glycosylase inhibitor (UGI), yielding a protein complex, referred to as base editor (BE), which is able to mediate direct conversion of C to T (or G to A) in human cell lines (Komor et al., 2016) without causing DSBs or requiring DNA template as a donor (Kim et al., 2017b; Komor et al., 2016). Furthermore, base editing occurs with higher probability between the 4th and 8th bases of the nonbinding strand of the sgRNA, allowing for more precise and controllable editing.

Until now, we were only aware of three *in vivo* reports using base-editing approach in mice (Kim et al., 2017a; Rees et al., 2017; Yeh et al., 2018). This base-editing approach has been used *in vitro* to disrupt gene function in cell lines (Billon et al., 2017; Kuscu et al., 2017), which can be achieved if a premature protein translation stop codon (TAA, TAG and TGA) is introduced in frame as a result of base editing in codons CAA, CAG, CGA or TGG. In this case, loss-of-function gene mutants are produced. Such an approach is called CRISPR-stop (Billon et al., 2017; Kuscu et al., 2017). In addition, thanks to the specificity of altered base pairs, CRISPR-stop can target selectively the protein-coding or long non-coding RNAs, even if these happen to be at the same genomic locus (Billon et al., 2017). Recently, mutant zebrafish have also been generated using base-editing methods (Zhang et al., 2017). The power of using the CRISPR-stop approach in zygotes for single- and multi-gene screening mouse developmental genes represents potential waiting to be harnessed by the community.

In vivo loss-of-function, rather than gain-of-function studies, are the gold standard for proving the necessity of the function of a gene in developmental biology. However, a given gene frequently has multiple homologs that can sometimes compensate for its absence. In this case, it is necessary to inactivate multiple related genes in order to uncover their function. It is therefore of interest to establish efficient ways to disrupt multiple genes simultaneously. We tested the use of the CRISPR-stop base editing method to meet this need. For ease of phenotypic and functional analysis, we used the mouse inner ear auditory organ, the cochlea, as a platform to demonstrate the capabilities of the CRISPR-stop method.

The mouse cochlea resides in the ventral region of the inner ear. Its auditory epithelium, the organ of Corti, contains hair cells (HCs) and neighboring supporting cells (SCs) (Kelley, 2006). Atoh1, a bHLH transcription factor, is required in HC fate specification; indeed, *Atoh1*$^{-/-}$ mice lack all HCs (Bermingham et al., 1999),

[1]Institute of Neuroscience, CAS Center for Excellence in Brain Science and Intelligence Technology, Shanghai Institutes for Biological Sciences, Chinese Academy of Sciences, Shanghai 200031, China. [2]University of Chinese Academy of Sciences, Beijing 100049, China. [3]Guangxi University, Nanning 530004, Guangxi, China. [4]Department of Otolaryngology, Head and Neck Surgery, Ninth People's Hospital, Shanghai Jiao Tong University School of Medicine, Shanghai 200011, China. [5]Ear Institute, Shanghai Jiao Tong University School of Medicine, Shanghai 200011, China. [6]Shanghai Key Laboratory of Translational Medicine on Ear and Nose Diseases, Shanghai 200011, China. [7]Biology Department, University of Massachusetts Amherst, Amherst, MA 01003, USA. [8]Key Lab of Computational Biology, CAS-MPG Partner Institute for Computational Biology, Shanghai Institutes for Biological Sciences, Chinese Academy of Sciences, Shanghai 200031, China. [9]Collaborative Innovation Center for Genetics and Development, Fudan University, Shanghai 200032, China. [10]Shanghai Center for Bioinformation Technology, Shanghai Industrial Technology Institute, Shanghai 200032, China.
*These authors contributed equally to this work

‡Authors for correspondence (huiyang@ion.ac.cn; zhiyongliu@ion.ac.cn)

H.P., 0000-0001-7696-3434; S.L., 0000-0003-3438-1588; L.S., 0000-0001-5890-1774; Z.L., 0000-0002-9675-1233

Received 13 June 2018; Accepted 19 September 2018

Development (2018) 145, dev168906. doi:10.1242/dev.168906

whereas overexpression of *Atoh1* results in ectopic HCs (Gubbels et al., 2008; Kelly et al., 2012; Liu et al., 2012; Zheng and Gao, 2000). Moreover, two subtypes of cochlear HCs exist: three rows of outer hair cells (OHCs) and one row of inner hair cells (IHCs). Both OHCs and IHCs are crucial for hearing capacity but have different roles and express different proteins. For example, prestin, which is encoded by *Slc26a5*, is a lateral membrane protein exclusively expressed in OHCs (Liberman et al., 2002; Zheng et al., 2000). It powers the electromotility of OHCs, a central component of the mammalian cochlear amplification mechanism (Brownell et al., 1985; Liberman et al., 2002). Prestin-mediated electromotility can be readily assessed by the presence of nonlinear capacitance (NLC) using standard patch-clamp hardware (Bai et al., 2006). The nonlinear region of the NLC curve offers functional information about prestin, whereas the linear portion of the curve gives information about OHC size (Navarrete and Santos-Sacchi, 2006). Mutation of prestin causes significant hearing impairment in humans (Liu et al., 2003) and mice (Liberman et al., 2002). In contrast to the modulatory role of OHCs, IHCs are the primary sound receptors and express vesicular glutamate transporter 3 (vGlut3, also referred to as *Slc17a8*) and a calcium sensing protein, otoferlin (Li et al., 2018; Roux et al., 2006), both of which are not present in adult OHCs. Mutation of either *vGlut3* or otoferlin leads to severe deafness in mice and human (Ruel et al., 2008; Seal et al., 2008; Yasunaga et al., 1999). Because of their importance and well characterized function in the inner ear, we chose *Atoh1*, prestin, *vGlut3* and otoferlin as targets for CRISPR-stop gene editing.

In a first step, we successfully optimized our experimental procedures using *Atoh1* as proof-of-principle gene. Multiple sgRNAs for each gene were pre-tested through *in vitro* validation on injected zygotes; the most promising sgRNAs were chosen to be injected into zygotes that would eventually be implanted into pseudopregnant female mice. Our data suggest that the selection of two 'promising' sgRNAs (see Fig. S1 for quantitative definition of 'promising') together typically generate homozygous F0 mutant mice. Mosaic mutants did occur but at a low rate. Most importantly, we could also produce triple homozygous prestin, *vGlut3* and otoferlin mutants in F0 mice, showing that targeting multiple genes simultaneously is possible using CRISPR-stop. Hence, CRISPR-stop presents a feasible approach for studying the effects of concurrent loss-of-function mutations in three, and potentially more, genes. Furthermore, as the sgRNA and base editor 3 (BE3) are injected into a one-cell stage zygote, which in turn gives rise to all tissues and organs of the body, the CRISPR-stop approach can be used to target any mammalian organ, making it a flexible and broadly applicable method. In conclusion, CRISPR-stop is a powerful tool that enables the rapid screening of candidate genes; this brings to mammalian research the equivalent of the transformative high-throughput RNAi screening technology available in some non-mammalian model organisms (Liu et al., 2015).

RESULTS

Base editing of the *Tyr* gene in mice using CRISPR-stop

In this study, we used the base editor 3 (BE3) complex (Komor et al., 2016). BE3 has three components fused together: Cas9 nickase (nCas9), cytidine deaminase (APOBEC1) and uracil glycosylase inhibitor (UGI), as shown in Fig. 1A. BE3 is guided to a target DNA sequence by gene-specific sgRNA; the complex catalyzes a base conversion in the target gene, converting C to T or G to A (Fig. 1B). If base editing occurs in-frame of a protein-coding sequence, a stop codon can be prematurely introduced and disrupt gene function (Fig. 1C); this approach is referred to as CRISPR-stop and works reliably in various cell lines (Billon et al., 2017; Kuscu et al., 2017). It is a powerful approach for loss-of-function studies, especially when the functional domains of the protein of interest are unknown.

To test whether the CRISPR-stop approach could be applied to mice, we initially focused on the tyrosinase gene (*Tyr*, for pigmentation), as a loss-of-function mutation in this gene produces mice with a white coat (Zuo et al., 2017), which is an easy and convenient phenotypic readout of successful gene inactivation. To achieve this, we injected BE3 mRNA together with a single design of *Tyr* sgRNA into one-cell stage zygotes (Fig. 1D,E). In total, 48 zygotes were implanted into pseudopregnant females and 18 F0 mice were obtained. Thirteen out of 18 (72.2%) displayed white coats, suggesting the occurrence of homozygous *Tyr* mutations (Fig. 1H). DNA sequencing confirmed the introduction of a premature stop codon in *Tyr* as a result of a C-to-T conversion (Fig. 1F,G). Nevertheless, in the same litters, five out of 18 (27.8%) bore black or brown coats, indicating the lack of, or heterozygous, *Tyr* mutations (Fig. 1H).

Proof-of-principle test of CRISPR-stop in mouse cochlea

Building on the positive results from the *Tyr* experiment, we next wanted to test whether CRISPR-stop could be used to affect *in vivo* organ function. We chose the cochlea as a model organ and the *Atoh1* gene as an illustration. *Atoh1* is required for generating cochlear HCs, as indicated by the complete loss of all HCs in *Atoh1*$^{-/-}$ mice (Bermingham et al., 1999). Such a severe phenotype provided us with a clear and rapid readout of the occurrence of loss-of-function mutations in *Atoh1*. As injecting a single sgRNA led to 72.2% homozygous mutants in the *Tyr* experiment, we tested whether injecting multiple designs of sgRNAs simultaneously would boost the chances of successful base editing. To achieve this, we designed seven sgRNA variants targeting *Atoh1*. DNA-sequencing data from injected blastocysts indicated that three of these sgRNAs were permissive to base editing and were further used for the subsequent steps outlined below (Fig. 2A and Fig. S1).

We injected BE3 mRNA together with sgRNA3 (group 1), sgRNA3+1 (group 2) or sgRNA3+1+2 (group 3), and compared the resulting base edits across the three groups. To rule out any effects caused by injecting BE3 mRNA and sgRNA themselves, we also injected GFP (green fluorescent protein) sgRNA with BE3 mRNA into zygotes that served as a control or wild-type group (Fig. 2B,C). Notably, in our study, base editing occurred equally well across all cochlear turns and no differences among different turns were identified. As *Atoh1*$^{-/-}$ mice die immediately after birth (Bermingham et al., 1999), we analyzed cochlear samples from each group at embryonic day 18.5 (E18.5). Detailed information about samples of each group can be found in Fig. S2A. Briefly, we used whole-mount immunostaining of the cochlea with myosin VI (a HC marker) to determine the effectiveness of the method at disrupting *Atoh1*. The complete absence of myosin VI was taken as supporting evidence for the presence of a homozygous loss-of-function mutation in the *Atoh1* gene. Three categories of phenotypic outcomes were identified in these experiments. The first case consisted of complete HC loss, corresponding to an effective homozygous base editing, which we defined as 100% KO (knockout) (Fig. 2D). Cochlear sensory epithelium maintained Sox2 expression in spite of HC loss (Fig. 2E). In the second class of outcomes, HCs were observed but their numbers were greatly reduced; such a phenotype was defined as mosaic (Fig. 2F). This suggests that only a fraction of sensory progenitors experienced

Development (2018) 145, dev168906. doi:10.1242/dev.168906

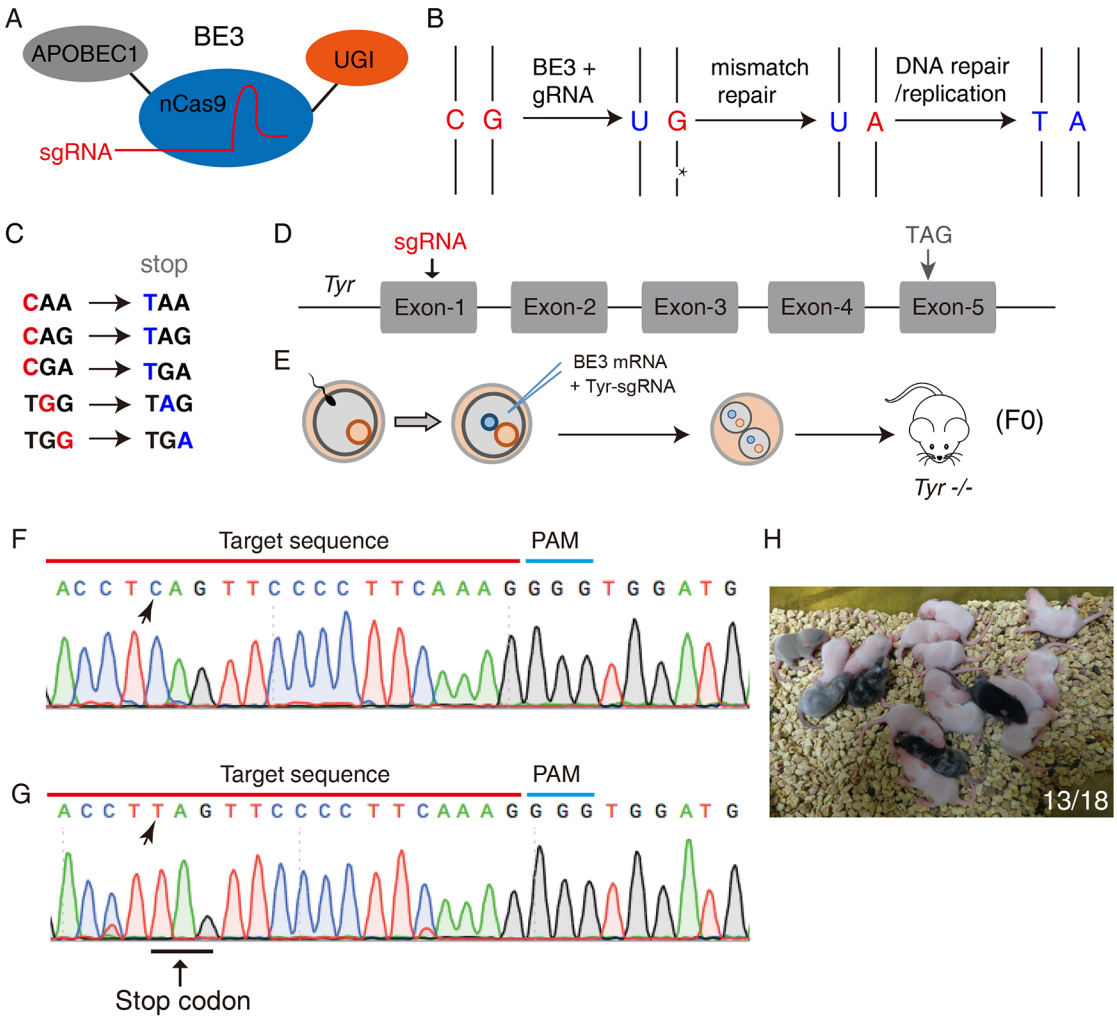

Fig. 1. Base editing in mouse *Tyr*. (A) Cartoon figure depicting the three components of the base editor 3 (BE3) complex with sgRNA. (B) Simplified mechanism underlying base editing of C to T (or G to A). Asterisk indicates a single-stranded DNA break. (C) Lists of common targeted codons whose base edit can lead to the premature appearance of a stop codon. (D,E) *Tyr* sgRNA targeting the first exon of the *Tyr* gene, along with BE3 mRNA was injected into one-cell stage zygotes; these zygotes were transplanted into pseudopregnant mice and developed into homozygous (F0) $Tyr^{-/-}$ mice. (F,G) An example comparison of Sanger DNA sequencing results between the *Tyr* wild-type (F) and mutant ($Tyr^{-/-}$) allele (G). Base C (arrow in F, position 5 in sgRNA) was converted into T (arrow in G), resulting in the appearance of a premature TAG stop codon (underlined in G). (H) Thirteen out 18 F0 mice had white coats, while the rest were either black or brown.

base editing. Finally, in the third case, HCs were distributed as in the wild-type cochlea, i.e. in four rows consisting of one IHC row and three OHC rows, suggesting that no *Atoh1* loss-of-function base editing had occurred in cochlear sensory progenitors. We defined such cases as wild-type like (Fig. 2G). Cochlear whole-mount myosin VI immunostaining demonstrated that group 2 (sgRNA3+1) produced consistent (100%) *Atoh1* homozygous mutants, and that mosaic mutations occurred only in group 1 (sgRNA3) samples (Fig. 2H). Owing to a lack of reliable Atoh1 antibody at hand, Atoh1 protein expression was not assessed.

To further confirm that base editing had occurred in the *Atoh1* gene, DNA Sanger sequencing of inner ear tissues was performed. The results showed that base C (arrow in Fig. 2I) had been converted to T (arrow in Fig. 2J), leading to the coding CAG being changed to TAG, a stop codon. We also performed next-generation deep sequencing to quantify the percentage of targeted C to T conversion among all cells dissected from inner ear tissues (Fig. 2K). The effectiveness of sgRNA3 in group 1 was 73.2±4.7% (n=18, mice number). In group 2, sgRNA3 caused 90±4.0% and sgRNA1 resulted in 44.4%±16.2% base editing (n=7, mice number). In group 3, the effectiveness of sgRNA3 was 76.9%±9.8%, sgRNA1 was 25.9%±6.7% and sgRNA2 was 36.1%±11.2% (n=10, mice number). Furthermore, for group 3 samples, we also performed TA cloning of PCR products covering all three sgRNAs-targeted sites. The data suggested that base editing occurred in the same allele (Fig. S2B). Taken together, the results show that introducing multiple sgRNAs can lead to non-additive gene disruption and increase the chances of loss-of-function gene mutations. Indeed, despite neither sgRNA alone being 100% effective, the combination of two sgRNAs in group 2 was sufficient to disrupt all *Atoh1* translation.

CRISPR-stop can efficiently generate different viable mouse models of severe deafness

Next, we focused on determining whether CRISPR-stop could be used to generate various deafness mouse models. Prestin-, *vGlut3*- and otoferlin-null mice all survive to adulthood and exhibit severe hearing loss (Liberman et al., 2002; Roux et al., 2006; Ruel et al.,

Development (2018) 145, dev168906. doi:10.1242/dev.168906

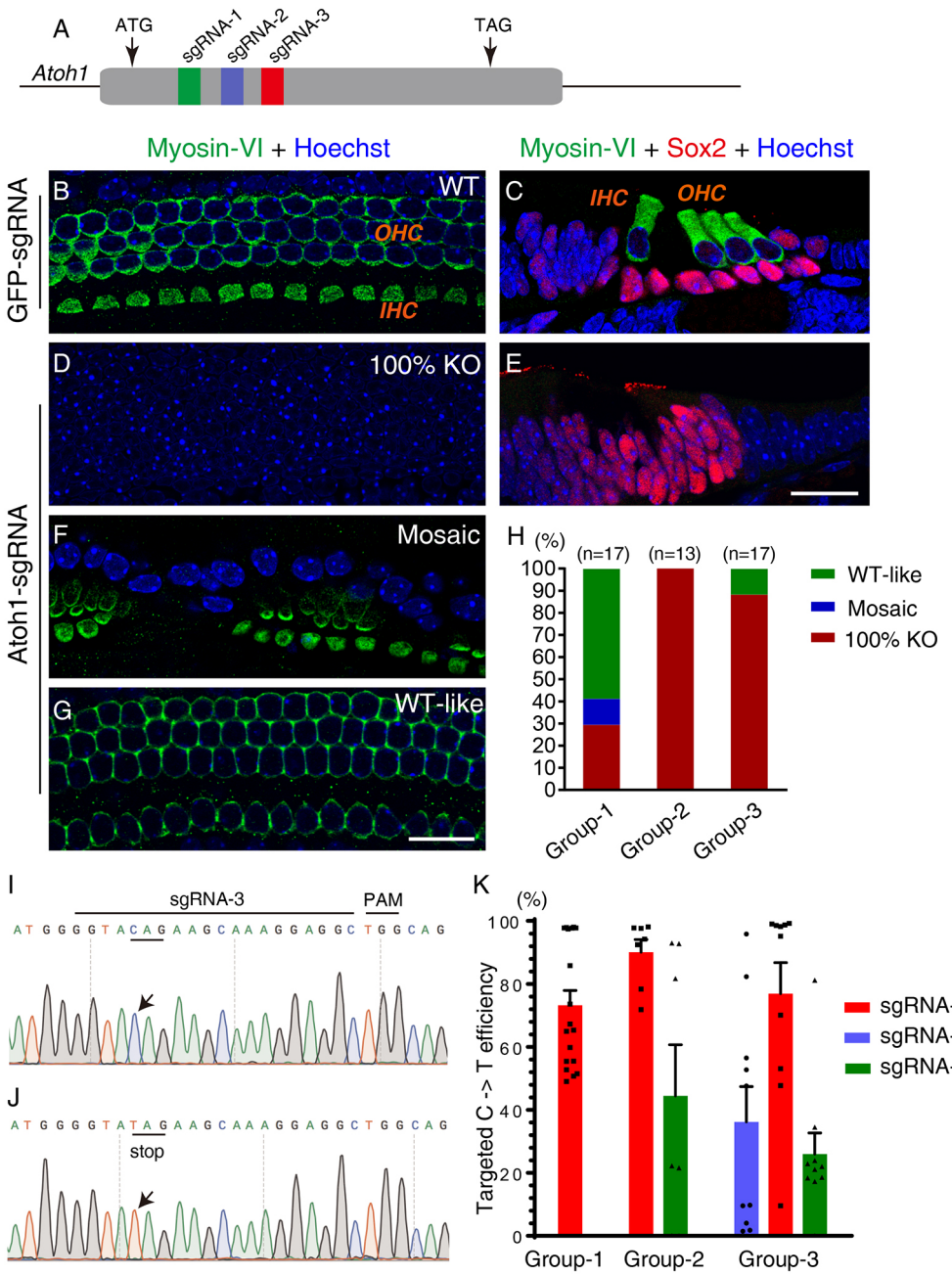

Fig. 2. Base editing in mouse *Atoh1*. (A) *Atoh1* has a single exon; three sgRNAs were designed close to the ATG start codon. (B,C) Whole-mount (B) or cryo-sectioned (C) wild-type cochlear samples were dissected from mice (E18.5) derived from *GFP*-sgRNA/BE3-treated zygotes and stained for myosin VI alone or also for Sox2. Three rows of OHCs and one row of IHCs were observed. (D,E) Whole-mount (D) or cryosectioned (E) cochlear samples were dissected from mice (E18.5) derived from *Atoh1*-sgRNA/BE3-treated zygotes and stained for myosin VI alone or also for Sox2. 100% knockout phenotype samples were defined as lacking all hair cells (HCs) (D); Sox2 expression was maintained (E). (F) Mosaic phenotypes were defined as those with sparsely distributed HCs; in these samples, derived from *Atoh1*-sgRNA/BE3-treated zygotes, the total number of HCs was reduced. (G) Wild-type-like phenotypes consisted of intact HCs, implying that, in these mice, derived from *Atoh1*-sgRNA/BE3-treated zygotes, loss-of-function base editing had not occurred. (H) Distribution of different phenotypes, 100% knockout, mosaic and wild-type like from each experimental group. Group 1 mice were injected with sgRNA3 only, group 2 mice were given sgRNA1 and sgRNA3, and group 3 mice were injected with sgRNA1, sgRNA2 and sgRNA3. All samples were stained using myosin VI antibody to visualize and quantify HCs to determine the effectiveness of base editing. All cochlear samples in group 2 lost HCs, indicating that the combination of two sgRNAs was, in this case, optimal. (I,J) DNA Sanger sequencing comparison between *Atoh1* wild-type (I) and mutant (*Atoh1* KO) alleles (J). Base C (arrow in I, position 5 in sgRNA3) was converted into T (arrow in J), leading to the premature appearance of a TAG stop codon (underlined in J). (K) Quantification of targeted C-to-T editing efficiency of three groups. Each circle/square/triangle represents the percentage of targeted base edits in each mouse. Bars are mean and error bars indicate the s.e.m. Scale bars: 20 µm.

2008; Seal et al., 2008). We therefore selected them as candidate genes to generate deaf mice using the CRISPR-stop approach. Based on the findings of the *Atoh1* study above, for every gene targeted, the two most promising sgRNAs were injected together. Again, GFP sgRNA was used to generate wild-type control mice. Samples were analyzed at 4 weeks of age and three categories of

Development (2018) 145, dev168906. doi:10.1242/dev.168906

phenotype were defined as before: 100% knockout, mosaic and wild-type like.

We first confirmed that vGlut3 was exclusively expressed in IHCs (within the dotted lines in Fig. 3A,A′) in wild-type group (n=3, mice number), consistent with our previous report (Li et al., 2018). *vGlut3* has 12 exons and its endogenous stop codon TAA is located within exon 12. From the pre-tested sgRNAs targeting *vGlut3*, the two most effective ones were found to target exon 3 and exon 8, respectively. In total, 19 zygotes were injected with BE3 mRNA and these two sgRNAs, and transplanted into pseudopregnant mice; 12 mice were born (Fig. S3A). Double staining of parvalbumin (Pvalb) and vGlut3 showed that 10 mice (83.4%) were 100% knockout (Fig. 3B,B′), one (8.3%) was mosaic (inset in Fig. 3B) and one (8.3%) was wild-type like (Fig. 3G). Otoferlin, in similar fashion to *vGlut3*, is selectively expressed in IHCs in wild-type mice (dotted lines in Fig. 3C,C′). The otoferlin gene consists of 47 exons, and its endogenous stop codon, TGA, is located within exon 46. In light of this, we designed two sgRNAs targeting exons 7 and 19. We transplanted 20 zygotes and obtained eight mice (Fig. S3A). Co-staining for myosin VI and otoferlin showed that all of the seven mice analyzed were 100% knockout (Fig. 3D,D′). Taken together, this demonstrates the efficient use of the CRISPR-stop method to generate loss-of-function mouse lines for two IHC-specific genes: *vGlut3* and otoferlin.

Contrary to *vGlut3* and otoferlin, prestin is exclusively expressed in OHCs in wild-type mice (Fig. 3E,E′). The prestin gene consists of 20 exons; the last exon contains its endogenous stop codon, TAA. We designed two sgRNAs targeting exons 4 and 11. In total, 20 zygotes were transplanted and 15 mice were born (Fig. S3A). Co-antibody staining for myosin VI and prestin demonstrated that among all 11 mice that we could analyze, seven (63.6%) were 100% knockout (Fig. 3F,F′) and four (36.4%) were mosaic (inset in Fig. 3F). To further confirm design-specific base-editing mutations, we amplified tail-DNA fragments covering the sgRNA target sites from each mutant model; in all cases, the sequencing data clearly showed a targeted C-to-T conversion (Fig. S3B).

To assess the hearing capacity of the mutant mice, we performed auditory brainstem response (ABR) analysis in the *vGlut3*, otoferlin

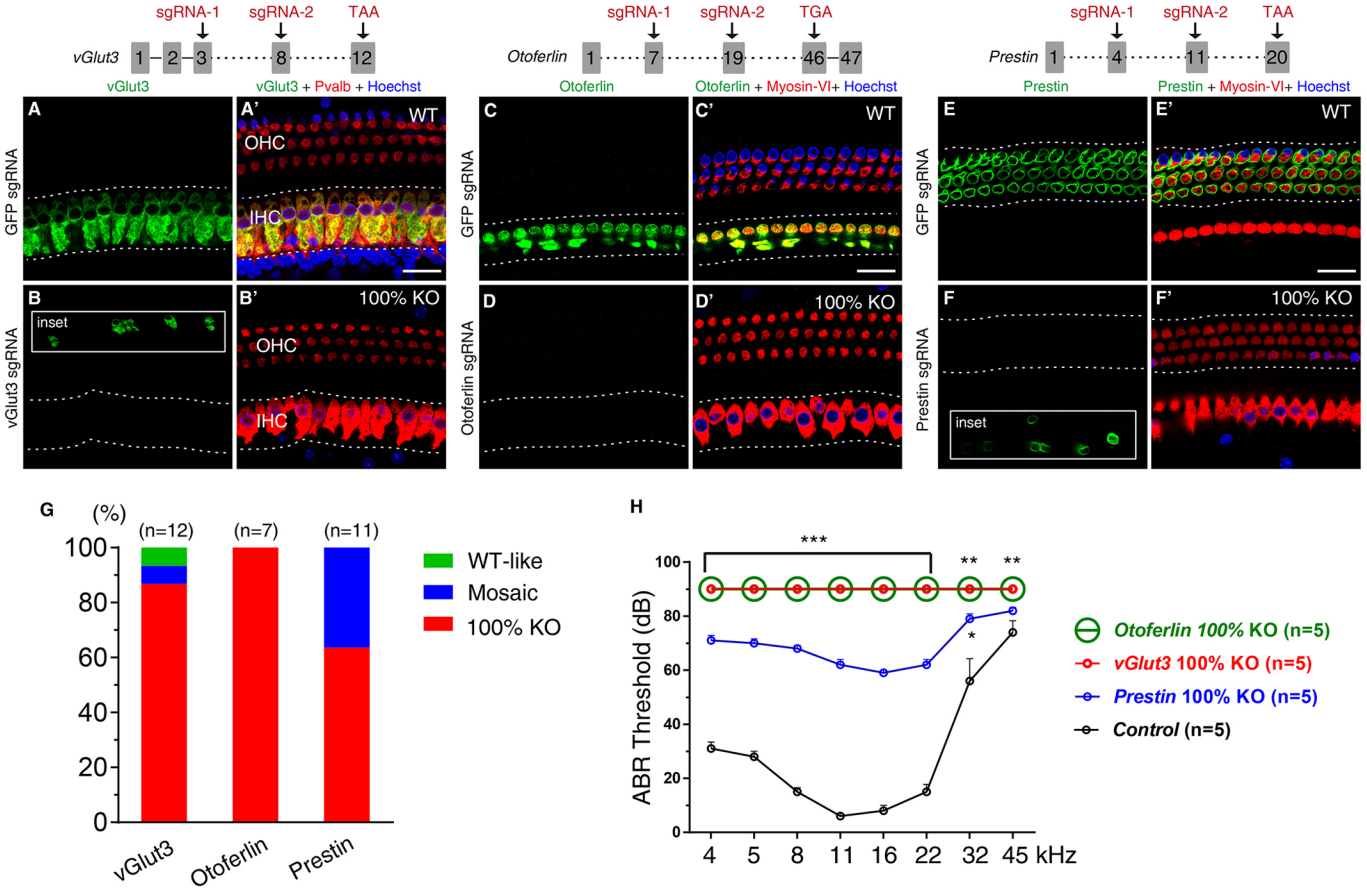

Fig. 3. Single gene base editing of mouse *vGlut3*, otoferlin and prestin. (A-B′) Whole-mount cochlear samples were stained for parvalbumin (Pvalb, a hair cell marker) and vGlut3. In the wild-type group (A,A′), Pvalb was expressed in both inner hair cells (IHCs) and outer hair cells (OHCs), while vGlut3 was expressed in only IHCs (within the dotted lines). In contrast, in cochleae (B,B′, 100% knockout) derived from zygotes receiving two *vGlut3* sgRNAs/BE3 mRNA, vGlut3 was absent from IHCs (within the dotted lines in B), while Pvalb expression was unchanged. The inset in B exemplifies the mosaic phenotype in which not all IHCs lost vGlut3. (C-D′) Similarly to vGlut3, in the wild-type group (C,C′), otoferlin was, as expected, exclusively expressed in IHCs (within the dotted lines). Myosin VI was expressed in both IHCs and OHCs. In otoferlin mutants (D,D′, 100% knockout), otoferlin was undetectable in IHCs (within the dotted lines); however, myosin VI expression pattern was left unchanged. (E-F′) Prestin was expressed in OHCs (within the dotted lines) in the wild-type group as expected (E,E′). In prestin mutants (F,F′, 100% knockout), all myosin VI$^+$ OHCs (within the dotted lines) lacked prestin expression. The inset in F exemplifies the mosaic phenotype in which not all OHCs lost prestin. (G) Quantification of different phenotypes caused by CRISPR-stop in *vGlut3*, otoferlin and prestin mutants. (H) The auditory brainstem response (ABR) measurement of each mutant. Compared with the control wild-type group (black line), *vGlut3*, otoferlin and prestin mutants showed significant hearing impairment across all frequencies, with the exception of the prestin mutant at 45 kHz (P=0.1). ***P<0.001, **P<0.01, *P<0.05. Data are mean±s.e.m. Scale bars: 20 µm.

Development (2018) 145, dev168906. doi:10.1242/dev.168906

and prestin mutants. In order to pre-select mice belonging to the 100% knockout category, we sequenced tail DNA and chose animals who showed the most effective targeted C-to-T conversion (Fig. 3B,B′,D,D′,F,F′). Compared with control mice (n=5), each mutant mouse (n=5) displayed a significantly increased ABR threshold, indicating severe deafness (Fig. 3H). In addition, *vGlut3* and otoferlin mutants exhibited a higher ABR threshold than the prestin mutant mice, consistent with previous reports (Liberman et al., 2002; Roux et al., 2006; Ruel et al., 2008; Seal et al., 2008).

Prestin and otoferlin mutants also have defective electrophysiological properties

Besides ABR measurement, we also performed electrophysiological analysis of prestin and otoferlin mutant mice. As before, we selected mice in the 100% knockout category using tail-DNA sequencing. Nonlinear capacitance (NLC) is a surrogate measurement used to assess the electromotility function of OHCs (Santos-Sacchi, 1991). As expected, NLC was absent in prestin 100% knockout mice (Fig. 4A). In addition to lack of electromotility, OHCs in prestin mutants showed significantly reduced linear capacitance, C_{lin}=4.01±0.26 (n=5, OHC numbers) when compared with control OHCs, C_{lin}=6.75±0.23 (n=7 OHCs) (Fig. 4B). This suggests that the lack of prestin results in smaller OHCs, consistent with previous reports (Abe et al., 2007; He et al., 2010; Liberman et al., 2002).

Otoferlin is a calcium-sensor protein and controls membrane fusion and exocytosis (Pangršič et al., 2010). To test for any changes in exocytosis of otoferlin mutant IHCs, we performed whole-cell patch-clamp recordings of IHCs and applied voltage steps of 10 ms to 1 s duration to induce exocytosis. We calculated the change in capacitance before and after stimulation (ΔC_m), and found that ΔC_m was greatly reduced in otoferlin mutant mice (upper panel in Fig. 4C). For depolarization of 500 ms, ΔC_m was significantly reduced (P<0.001) from 392±113 fF (n=12, IHC cell number, control) to 34.3±10.6 fF (n=9 IHCs, otoferlin mutant). Meanwhile, Ca^{2+} influx (Q_{Ca}) was not significantly changed, being −55.7±5.36 pC for control and −41.5±7.73 pC for otoferlin knockout (lower panel in Fig. 4C). These results are highly consistent with previously published otoferlin mutant models (Moser and Beutner, 2000; Roux et al., 2006) and provide further evidence supporting the absence of prestin and otoferlin proteins in prestin and otoferlin mutant mice, respectively.

In summary, the DNA sequencing, immunostaining and functional analysis data show that CRISPR-stop successfully induced *in vivo* loss-of-function of two IHC-specific genes and one OHC-specific gene. The observed efficiency of the method 63.6-100% (Fig. 3G) is highly promising. Our results highlight the power of the CRISPR-stop method to rapidly and efficiently generate mouse deafness models.

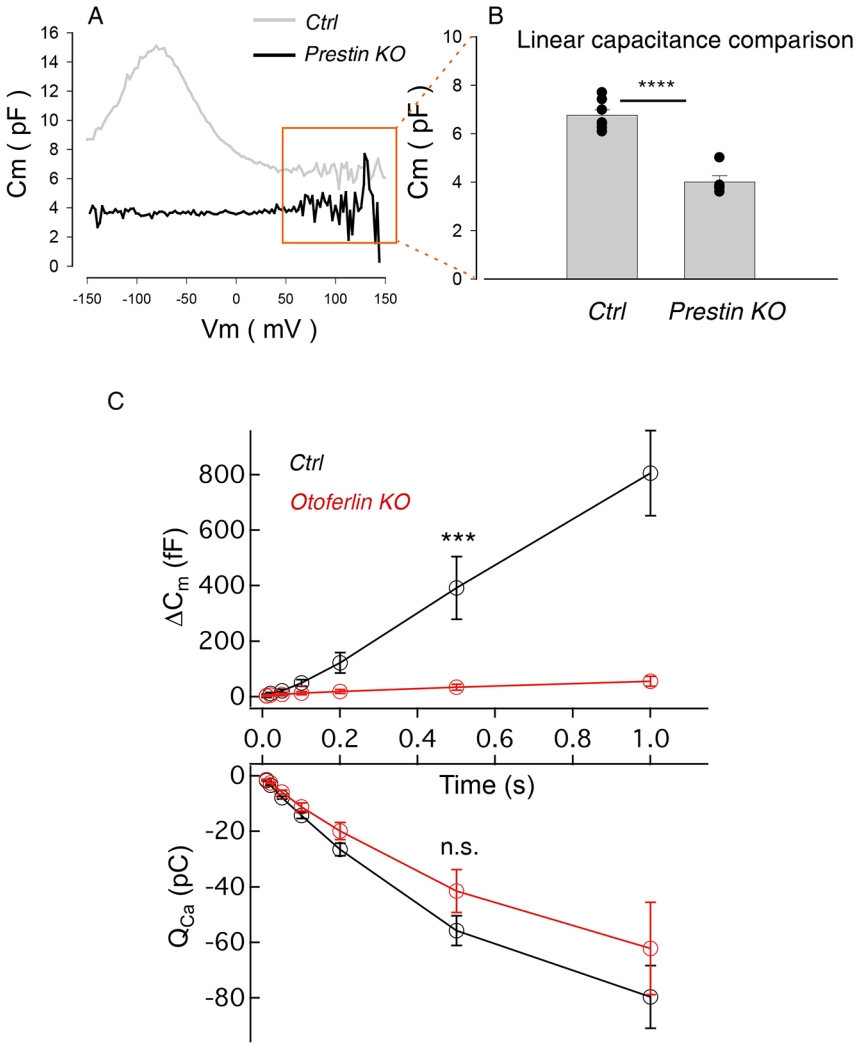

Fig. 4. Patch-clamp measurement of OHCs and IHCs in prestin and otoferlin mutants, respectively, at 4 weeks of age. (A) Nonlinear capacitance (NLC) functions were measured in both prestin knockout and wild-type control (*Ctrl*) OHCs. The gray line is a representative example of a trace from a control OHC, which showed a typical nonlinear capacitance pattern. This was absent in prestin knockout OHCs (black line). (B) Comparison of linear capacitance (C_{lin}) between control and prestin knockout. The 'linear region' used for this analysis is shown by the orange square in A. C_{lin}=6.75±0.23 (n=7, control); C_{lin}= 4.01±0.26 (n=5, prestin knockout). OHCs in prestin knockout mice had a smaller C_{lin}, a previously reported indicator of reduced cell size. ****P<0.0001. Data are mean±s.e.m. Circles represent individual data points. Q_{max}=1.09±0.04; V_h=-61.5±5.5; Z=0.95±0.01. These three parameters are only applicable to control OHCs. (C) Step depolarization-evoked capacitance jump (ΔC_m, upper) and Ca^{2+} influx (Q_{Ca}, lower) in IHCs of control (black) and otoferlin knockout (red) mice. ΔC_m was largely abolished in otoferlin knockout mice (***P<0.001) whereas Q_{Ca} was not significantly changed (P>0.05, t-test). The data are mean±s.e.m. n.s., non-significant difference.

Development (2018) 145, dev168906. doi:10.1242/dev.168906

CRISPR-stop can lead to simultaneous inactivation of three genes

Encouraged by the high efficiency of CRISPR-stop at inactivating single genes in our pilot experiments described above, we next proceeded to determine whether we could inactivate *vGlut3*, otoferlin and prestin simultaneously. Control mice were derived from zygotes that were injected with GFP sgRNA and BE3 mRNA, and we confirmed the expression of vGlut3 and otoferlin in IHCs and prestin in OHCs in this control group (Fig. 5A-A‴). The same six sgRNAs (two per gene) used in the previous studies were injected together with BE3 mRNA into one-cell stage zygotes and produced triple homozygous mutant F0 mice (Fig. 5B-B‴). When compared with the dose of sgRNAs given during the individual gene mutation experiments (Fig. 3), we doubled the dose of each sgRNA in order to increase the probability of generating 100% triple knockout and decrease the incidence of mosaic and wild-type-like cases. In total, 40 zygotes were transplanted and 15 mice were born. All mice but one were found to be 100% triple knockout, showing no expression of vGlut3, prestin or otoferlin (Fig. 5B-C). One of the 15 exhibited mosaic prestin expression (inset in Fig. 5B′). To confirm that cells counterstained by Hoechst were HCs (within dotted lines in Fig. 5B‴), half of any single cochlea was stained for myosin-VI, prestin and otoferlin (Fig. S4A-B‴), while the other half was stained for parvalbumin (Pvalb), vGlut3 and prestin (Fig. S4C-D‴). This combinatorial approach permitted us to perform five-antibody staining in any single cochlea, allowing us to identify HC identity, via myosin-VI or Pvalb staining, while also being able to assess the presence of two other proteins of interest. These data also show that HCs (myosin-VI$^+$ or Pvalb$^+$) can survive regardless of the concurrent absence of vGlut3, otoferlin and prestin (Fig. S4B,D).

To further rule out the possibility that disrupting any one gene (e.g. *vGlut3*) could lead to the inactivation of the other two genes through pathways other than direct base editing, we stained single mutant mice with antibodies against the other two proteins (e.g. staining for otoferlin and prestin in *vGlut3* mutants) (Fig. 5D-F′‴).

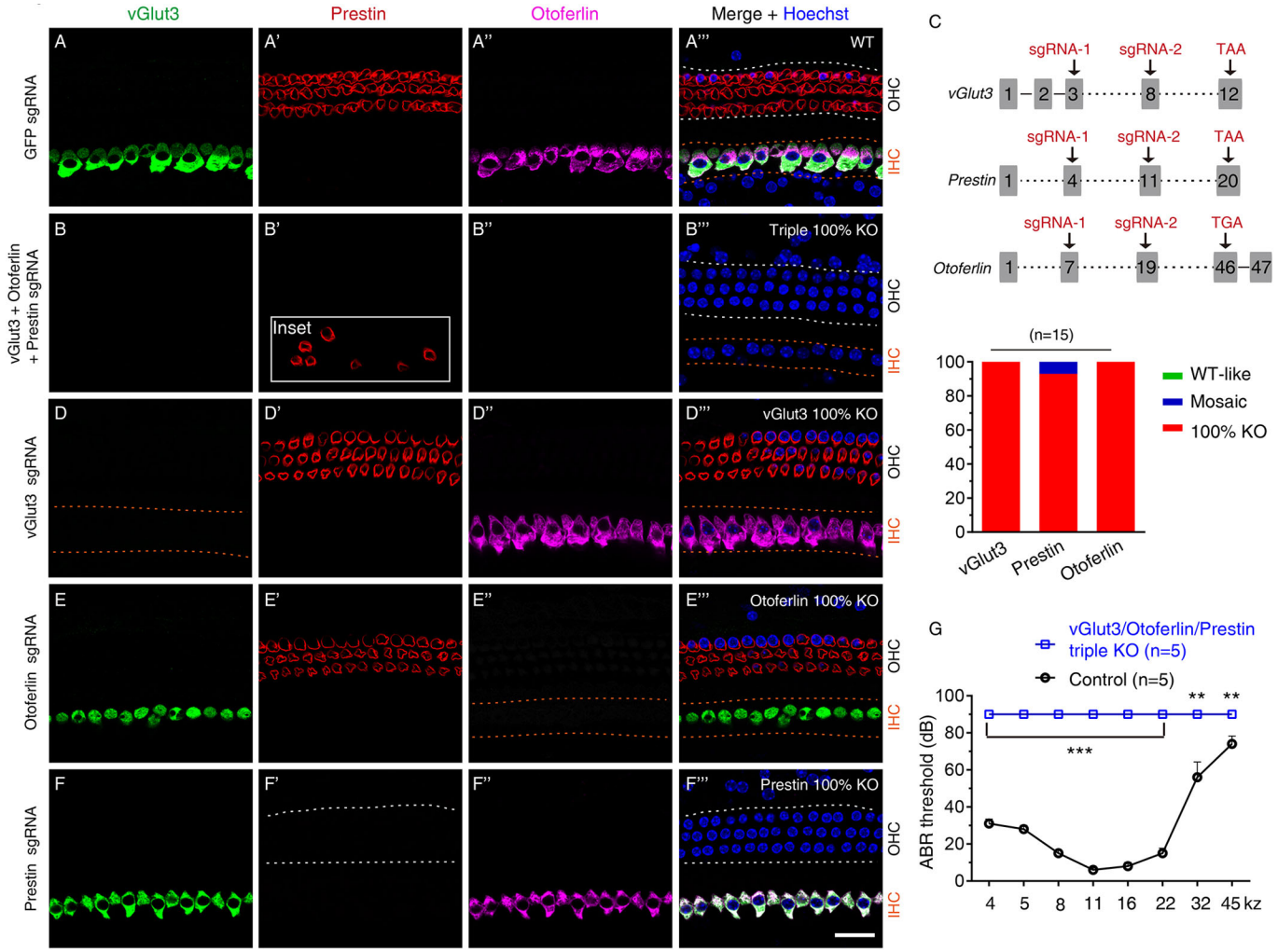

Fig. 5. Simultaneous base editing of *vGlut3*, otoferlin and prestin. (A-B‴) Triple antibody staining against vGlut3, otoferlin and prestin in the wild-type group (A-A‴) and triple 100% knockout group (B-B‴). White dashed lines outline the OHCs; orange dashed lines outline the IHCs. The inset in B′ is one of the triple mutant cochlear samples that had mosaic prestin expression. (C) Quantification of protein expression of each gene in triple mutants. All but one of the 15 mice analyzed lost expression of vGlut3, prestin and otoferlin; the outlier exhibited mosaic prestin expression (inset in B′). (D-F‴) Triple co-staining against vGlut3, otoferlin and prestin in *vGlut3* mutant (D-D‴), otoferlin mutant (E-E‴) and prestin mutant (F-F‴) groups. Mutations in either gene alone did not affect the expression pattern of the other two genes. (G) Auditory brainstem response (ABR) measurement of triple mutant F0 mice. Compared with the control wild-type group (black line), in all frequencies, triple mutants (blue line) showed significant hearing impairment. ***P<0.001, **P<0.01. Data are mean±s.e.m. Scale bars: 20 µm.

Development (2018) 145, dev168906. doi:10.1242/dev.168906

We found that disruption of any individual gene did not affect expression of the other two genes (Fig. 5D-F‴). Finally, we performed ABR measurement and *vGlut3*/otoferlin/prestin triple mutant mice were completely deaf (Fig. 5G). Taken together, these findings demonstrate that CRISPR-stop is effective at simultaneously disrupting *vGlut3*, otoferlin and prestin.

No off-target effects were observed in *vGlut3*, otoferlin and prestin triple mutants

To quantify on-target efficiency of base editing more precisely and also reveal any potential genome-wide off-target effects from the six injected sgRNAs (two sgRNAs per gene), we performed next-generation whole-genome sequencing (WGS) at an average depth of 20× on three triple mutant mice (numbers 1, 5 and 8) (Fig. S5A). With regards to the on-target analysis, we confirmed that the efficiency of *vGlut3* and prestin sgRNAs targeted locations was 100% (all reads contained base editing) in all three mice (Fig. S5A). For the otoferlin-targeted positions, mouse number 8 base editing showed 100% efficiency. Mice 1 and 5 showed some heterogeneity in sgRNA target site base-editing efficiency: 14/18 (77.8%) and 100% at otoferlin sgRNA1 targeted position; and 100% and 15/21 (71.4%) at otoferlin sgRNA2 targeted position (Fig. S5A) for mice 1 and 5, respectively.

We next estimated off-target effects by identifying single nucleotide variations (SNVs) and insertions and deletions (indels) at these locations. After filtering variants located in genome complex regions, no SNVs or indels were detected within the predicted off-target sites, suggesting high specificity of the selected sgRNAs (Fig. S5B). Together, these results show that the silencing of three genes using two sgRNAs per gene was both efficient and specific.

In summary, we tested the CRISPR-stop approach *in vivo* and successfully generated five homozygous gene disruptions in F0 mice in *Tyr*, *Atoh1*, *vGlut3*, otoferlin and prestin. Importantly, we were also able to disrupt three genes simultaneously. The method is ideal to generate compound gene mutations; furthermore, three is unlikely to be an upper limit on the number of possible genes that can be simultaneously disrupted. As the F0 mutant mice produced are homozygous mutants for one or multiple genes, laborious mouse colony breeding work can effectively be bypassed. We foresee that the CRISPR-stop method will become a game-changer for the development of high-throughput genetic screening of mice and potentially other mammals.

DISCUSSION

In this pilot *in vivo* study, we demonstrate, step-by-step, the powerful ability of the BE3-CRISPR-stop method to efficiently generate F0 homozygous loss-of-function mouse mutants for individual or combinations of different genes (*Tyr*, *Atoh1*, *vGlut3*, otoferlin and prestin). As detailed above, CRISPR-stop works by inducing targeted C-to-T or G-to-A conversion that can introduce a premature stop codon into a protein-coding sequence, providing an effective way of generating loss-of-function mutants. Deciding which exons should be mutated in a target gene can be challenging, especially when working with large proteins of unknown functions. CRISPR-stop overcomes this challenge by allowing the user to design sgRNA targeting regions closer to the ATG start codon (Kuscu et al., 2017). Furthermore, coding genes are sometimes also involved in producing non-coding RNAs transcribed in the opposite direction. CRISPR-stop can selectively disrupt coding genes by inducing only C-to-T or G-to-A point mutations, thereby maximally keeping non-coding genes intact (Billon et al., 2017).

Genetic loss of function is a gold standard in proving the importance of a gene and understanding its physiological role. However, genomes often have multiple homologous genes that can interact. As a result, compensation frequently occurs in response to the deletion of any one of them, potentially masking important functional roles of genes. Generating gene mutants one by one followed by cross-breeding is laborious and time consuming. Using three genes that are crucial to normal hearing function, *vGlut3*, otoferlin and prestin as examples, we showed that these three genes can be simultaneously mutated. Notably, we showed that triple homozygous F0 mutant mice can be obtained within 19 days of injecting zygotes with sgRNAs and BE3 mRNA, making them ready for histological and functional analysis 1 month later. Generation of targeted compound mutants has never been achieved at this speed before. Single or triple mutant F0 mice can also produce F1 mice for future breeding if necessary. We believe that this method will benefit and have significant impact on many fields of developmental biology, including auditory neuroscience.

We also note that some gene mutations can be embryonically or perinatally lethal. Generating a mouse model with mosaic gene mutation through CRISPR-stop can potentially resolve lethality problems and avoid laborious mouse breeding when using tissue- or cell-specific Cre/Loxp-mediated conditional knockout approaches. Mosaic mouse mutants can be generated via two alternative approaches: the first approach consists of using either single sgRNA or multiple low-efficiency sgRNAs in order to achieve higher occurrence of mosaic mutations, as we described above; the second approach involves inducing base editing in only one cell of two-cell stage zygotes, instead of the usual one-cell stage zygotes. This ensures that organs will comprise cells of mixed progeny (wild type or mutant) derived from either of the two initial cells. The latter approach proved successful in a recent report where *Tet3* functions were illustrated in the mosaic mutant (Wang et al., 2017). Although this is still an on-going study, we can obtain *Atoh1*$^{-/-}$ mosaic mice that survive until at least postnatal day 7 (P7). Looking towards the future, we plan to further explore the potentials of mosaic mutant analysis to uncover yet-unknown functions of inner ear developmental genes.

Besides genetic loss-of-function studies, CRISPR-based technology is widely used for gene therapy. The CRISPR-stop method can also be potentially used for gene therapy, as exemplified in the case of TMC1, a putative mechanosensory transduction channel (MET) protein, the dominant-negative mutation of which impairs hearing (Vreugde et al., 2002). Inactivation of this dominant-negative mutation, using CRISPR paired with a sgRNA that can distinguish the wild-type from the mutant allele, results in reduced progressive hearing loss and higher HC survival rate (Gao et al., 2018). Moreover, one previous report estimated there to be 300-900 clinical relevant known human genetic diseases caused by point mutations, such as hearing impairment induced by an otoferlin point mutation (3413T to C), CIB2 (368T to C), TMC1 (1543T to C), CDH23 (5663T to C) and GJB2 (269T to C) (Komor et al., 2016). Fortunately, such T-to-C point mutation has an appropriate *NGG* PAM sequence nearby and can be rescued by CRISPR-stop. For point mutations without the appropriate *NGG* PAM sequence nearby, future x-Cas9-based CRISPR-stop may provide an alternative (Hu et al., 2018). For other types of mutations with a premature stop codon mutation, such as Duchenne muscular dystrophy, adenine base editors (ABEs), which trigger A-to-G conversion, represent potential solutions (Ryu et al., 2018).

In summary, our data demonstrate that CRISPR-stop works robustly in mouse zygotes *in vivo* and can produce viable genetic

Development (2018) 145, dev168906. doi:10.1242/dev.168906

mutants. Single or compound F0 mutant mice can be efficiently generated, making them rapidly available for further analyses. This has the potential to significantly speed up *in vivo* genetic mouse screening, matching the efficiency of *Drosophila* screening technology. Injection of base editing complexes into neonatal cochlea for gene manipulation was recently reported (Rees et al., 2017; Yeh et al., 2018). In future, CRISPR-stop has the potential to be used to correct T-to-C point mutations in various human disease models, including deafness.

MATERIALS AND METHODS

Base editor 3 (BE3) mRNA and sgRNA synthesis

Three steps were needed for *in vitro* synthesis of BE3 mRNA. First, the PCR amplicon (5543 bp) was obtained by using pCMV-BE3 (Addgene, 73021) as template with forward primer (5′-3′) TCCGCGGCCGCTAATACGACT and reverse primer (5′-3′) CACACAGGAAACAGCTATGACCATG, and KOD-plus-neo kit (TOYOBO, KOD-401), followed by purification with MinElute PCR purification kit (Qiagen, 28004). Second, the 5543 bp DNA amplicon (100 ng/µl) was used as template for *in vitro* transcription with mMACHINE T7 Ultra kit (ThermoFisher Scientific, AM1345). Third, transcribed mRNA was further purified with MEGAclear Transcription Clean-Up Kit (Ambion, AM1908) and the concentration was adjusted to 500 ng/µl with RNase-free water (Thermo Fisher Scientific, AM9937). Finally, aliquots of BE3 mRNA (1 µl/tube) were saved and kept at −80°C.

A similar approach was used for each individual sgRNA synthesis. First, vector pX330 (Addgene, 42230) was used as template to obtain amplicon (120 bp) with KOD-plus-neo kit (TOYOBO, KOD-401). The same reverse primer (5′-3′) AAAAGCACCGACTCGGTGCC was used for all genes. However, the forward primer (5′-3′) was different for each gene and it was composed of three parts: TAATACGACTCACTATAGG+sgRNA (20 bp)+GTTTTAGAGCTAGAAATAG. Only the middle part needed to be changed, depending on each specific gene. Second, the PCR amplicon, which was purified with MinElute PCR Purification Kit (Qiagen, 28004) and adjusted to 150 ng/µl, was transcribed *in vitro* with MEGA shortscript T7 kit (ThermoFisher Scientific, AM1354). Third, the transcribed sgRNAs were purified with MEGAclear Transcription Clean-Up Kit (Ambion, AM1908). The sgRNA concentration was adjusted with RNase-free water to 250 ng/µl (for a single gene mutant) or 1000 ng/µl (for triple gene mutants); 1µl aliquots were dispensed and stored at −80°C. The quality of the *in vitro* transcribed mRNA is key for successful base editing. A clean PCR workstation (AirClean Systems, 600 model) is recommended, as well as the use of RNaseZap Decontamination Solution (ThermoFisher Scientific, AM9780).

The sgRNA optimization, mouse inner ear/tail genotyping, targeted deep sequencing and TA cloning sequencing

For each gene base editing, we chose four to seven sgRNAs and tested them individually in one-cell stage zygotes dissected out from super-ovulated female C57BL/6 mice (4 weeks old) that were pretreated with PMSG and hCG, and crossed with C57BL/6 male mice. After injection of BE3 mRNA and sgRNAs, zygotes were cultured until blastocyte stage and DNA was extracted for nest PCR as the amount of blastocyte DNA was limited. Efficiency of the targeted base editing (C to T) was determined using Sanger DNA sequencing. All animal work conducted for this study was approved by the Institutional Animal Care and Use Committee at Institute of Neuroscience, Chinese Academy of Science and performed according to NIH guidelines.

The genotypes of gene-edited mice were determined by using PCR on genomic DNA extracted from mouse inner ears (*Atoh1*) or mouse tails (*vGlut3*, otoferlin and prestin). Both methods work well; in both cases, we found that the genotyping and phenotyping results matched perfectly. PCR primers were the same as the primers used in the sgRNA optimization step described above, with the exception that the nest PCR was no longer needed.

For *Atoh1*, targeted next-generation DNA-sequencing sites were amplified from genome DNA using Phanta Max Super-Fidelity DNA Polymerase (Vazyme Biotech). The paired-end sequencing of PCR amplicons was completed using Illumina HiSeq X Ten platform in CloudHealth Genomics. All primers for targeted deep sequencing are described in Table S1.

For the TA cloning of *Atoh1*, inner ear genomic DNA from three mice with 100% knockout phenotypes was used. PCR amplicons covering sgRNA1-3 were subcloned into TA cloning vector pMD19T (Takara) for sequencing analysis. Per inner ear DNA, 20 clones in total were analyzed, and targeted base editing patterns are summarized in Fig. S2B.

Zygote injection and embryo transplantation

For the single-gene base-editing experiments, we used BE3 mRNA (100 ng/µl) and sgRNAs (50 ng/µl for each sgRNA). For triple mutant experiments, sgRNA concentration was doubled (100 ng/µl) and BE3 mRNA was kept the same. BE3 mRNA and sgRNAs were mixed well and centrifuged. Using a FemtoJet microinjector (Eppendorf) with constant flow settings, supernatant of the mixed solution was injected into the cytoplasm of fertilized eggs with well-recognized pronuclei, in a droplet of HEPES-CZB medium containing 5 µg/ml cytochalasin B (CB). The injected zygotes were cultured for 1.5 days (until two-cell stage) in KSOM medium with amino acids at 37°C. Finally, two-cell embryos were transplanted into oviducts of pseudopregnant ICR females at 0.5 dpc. All pre-tested and promising sgRNAs used in this study are listed in Table S2.

Sample processing, histology and immunofluorescence

We followed our routine protocols described previously (Li et al., 2018; Liu et al., 2010). Briefly, after mice were perfused with 1×PBS and 4% PFA, inner ear tissue was dissected out and immediately placed into 4% PFA and kept at 4°C overnight. E18.5 mouse inner ear tissue was then washed with 1×PBS three times and then stored in 1×PBS at 4°C for cochlea dissection. Four-week-old mouse inner ear tissue was decalcified in EDTA for ∼2 days and subsequently washed with 1×PBS three times.

The following primary antibodies were used: anti-myosin VI (rabbit, 1:200, 25-6791, Proteus Bioscience), anti-Sox2 (goat, 1:1000, sc-17320, Santa Cruz Biotechnology), anti-prestin (goat, 1:200, sc-22692, Santa Cruz Biotechnology), anti-vGlut3 (rabbit, 1:500, 135203, Synaptic System), anti-parvalbumin (mouse, 1:1000, P3088, Sigma) and anti-otoferlin (mouse, 1:200, ab53233, Abcam). All secondary antibodies that were compatible with different combinations of primary antibodies were purchased from ThermoScientific. Following immunostaining, samples were counterstained with Hoechst33342 solution in PBS (1:1000, 62249, ThermoScientific) to visualize cellular nuclei. Samples were mounted with Prolong gold antifade mounting medium (P36930, ThermoScientific). All immunofluorescence images were examined using either a Nikon NiE-A1 plus confocal microscope, a Nikon TiE-A1 plus confocal microscope or a Nikon C2 confocal microscope.

Whole-genome sequencing and off-target analysis

Triple mutants of *vGlut3*, otoferlin and prestin mouse tail DNA were sequenced at the BGI company using Illumina HiSeq X Ten and DNA sequencing. Coverage depth was over 20×. Qualified reads were mapped to the mouse reference genome (mm10) by BWA (v0.7.12) with default parameters. The BAM files were then sorted and duplicates were marked using Picard 'MarkDuplicates'. Mutect2 was run on the aligned sequence files for variants detection. Single nucleotide variations (SNVs), and insertions and deletions (indels) were further filtered to exclude variants located in low-complexity regions, including UCSC repeat regions and microsatellite sequences. All of the mapped data are available from the Sequence Read Archive (SRA) under Accession Number SRP150150.

Potential off-target sites of sgRNAs were predicted as previously reported (Bae et al., 2014); further information can be found at www.rgenome.net/cas-offinder/. We extracted all off-target sites with no more than eight mismatches and two DNA or RNA bulges for each sgRNA.

Auditory brainstem response (ABR) measurement

The detailed protocols of ABR measurement have been described in our previous report (Li et al., 2018). For each condition, five mice (4 weeks of age) were tested at different frequencies: 4 kHz, 5 kHz, 8 kHz, 11 kHz,

Development (2018) 145, dev168906. doi:10.1242/dev.168906

16 kHz, 22 kHz, 32 kHz and 45 kHz. All frequencies were analyzed by two-way ANOVA followed by a Student's *t*-test with a Bonferroni correction. Both male and female mice were used for ABR measurement.

General patch-clamp preparation and procedure for preparing outer hair cells

Inner ear temporal bones were excised and cochleae dissected in 1×PBS solution. Excised apical turns from the organ of Corti were used for recording. Individual OHCs were confirmed by visualizing stereocilia from their apical region under a 40× water immersion lens. Surrounding supporting cells were removed with a large tip pipette. OHCs were then approached by applying positive pressure in the pipette. Pipette pressure was released when targeted OHCs were isolated. The extracellular solutions contained 132 mM NaCl, 2 mM $CaCl_2$, 2 mM $MgCl_2$ and 10 mM HEPES. Final solutions were adjusted to ∼300 mOsm with D-glucose and to pH 7.2∼7.3 with NaOH. The intracellular solution was the same as the extracellular solution except for the addition of 10 mM EGTA. Pipette impedance was ∼5-6 MΩ.

OHCs were recorded under whole-cell patch-clamp configuration at room temperature. An axon 200B amplifier was used for data collection. Non-linear capacitance (NLC) was measured using a continuous high-resolution (2.56 ms sampling) two-sine stimulus protocol (10 mV peak at both 390.6 and 781.2 Hz) superimposed onto a 300 ms voltage ramp from up to +160 to −160 mV (Song and Santos-Sacchi, 2013). All recordings and analysis were performed using jClamp (SciSoft, Ridgefield, CT, USA; www.scisoftco.com). Capacitance data were fitted to the first derivative of a two-state Boltzmann function (Santos-Sacchi, 1991), as follows:

$$C_m = Q_{\max}\frac{ze}{kT}\frac{b}{(1+b)^2} + C_{lin},$$

where

$$b = \exp\left(\frac{-ze(V_m - V_{pkCm})}{kT}\right).$$

The following notations were used: Q_{max}, maximum nonlinear charge moved; C_{lin}, linear membrane capacitance; V_{pkcm} or V_h, voltage at peak capacitance; V_m, membrane potential; z, valence; e, electron charge; k, Boltzmann's constant; T, absolute temperature. Averaged parameters were reported as mean±s.e.m. The *t*-test was used as statistical analysis to compare C_{lin} between wild-type control (*Ctrl*) and prestin knockout.

Inner hair cell patch-clamp and capacitance measurements

Apical cochlear turns were dissected out from control (Ctrl) and otoferlin knockout mice (pre-selected by tail-DNA sequencing at 4-5 weeks of age) in an external solution containing 130 mM NaCl, 2.8 mM KCl, 1.3 mM $CaCl_2$, 1 mM $MgCl_2$, 10 mM HEPES and 10 mM glucose (pH 7.40). Whole-cell patch-clamp recordings were performed in IHCs through a Heka EPC10/2 amplifier and the data were acquired on a PC running Heka Patchmaster. The pipette solution contained 135 mM Cs-methanesulfonate, 10 mM CsCl, 10 mM TEA-Cl, 10 mM HEPES, 2 mM EGTA, 3 mM MgATP and 0.5 mM NaGTP (pH 7.20). To increase the amplitude of Ca^{2+} currents, external Ca^{2+} was raised to 10 mM in experiments. IHCs were held at −90 mV and exocytosis was induced by depolarizing the membrane to −10 mV. Sinewaves of 1 kHz and 70 mV peak-to-peak amplitude were superimposed on the holding potential before and after stimulation, and capacitance measurements were extracted under the Sine+DC mode in Patchmaster (Moser and Beutner, 2000). The liquid junction potential was calculated to be ∼10 mV and was subtracted offline.

Acknowledgements

We thank Dr Qian Hu and the Optical Imaging Facility of the Institute of Neuroscience for support with confocal image capture and analysis, and Dr Virginia M. S. Rutten, HHMI-Janelia Research Campus (Ashburn, VA, USA) for polishing our written English.

Competing interests

The authors declare no competing or financial interests.

Author contributions

Conceptualization: H.Z., H.P., C.Z., H.Y., Z.L.; Methodology: H.Z., H.P., C.Z., Y.W., W.Y., G.W., G.L., X.D., Y.S., G-L.L., S.L., Y.L., H.Y., Z.L.; Validation: H.Z.; Formal analysis: H.Z., H.P., C.Z., S.L., G.W., C.L., Y.R., G.L., X.D., Y.S., G.-L.L., L.S., Z.L.; Investigation: H.Z., H.P., C.Z., S.L., G.W., C.L., Y.R., G.L., X.D., Z.L.; Writing - original draft: H.Z., G.L., L.S., H.Y., Z.L.; Writing - review & editing: H.Z., H.P., C.Z., Y.S., G.L., L.S., H.Y., Z.L.; Supervision: H.Y., Z.L.; Project administration: H.Y., Z.L.; Funding acquisition: L.S., H.Y., Z.L.

Funding

This study was supported by the Chinese Thousand Young Talents Program (Z.L.), by a Chinese National Science and Technology major project (2017YFA0103900/2017YFA0103901 to Z.L. and 2017YFC1001302 to H.Y.), by the Strategic Priority Research Program of the Chinese Academy of Sciences (XDBS01000000 to H.Y.), by a Shanghai City Committee of Science and Technology project (16JC1420202 to H.Y.), by the National Natural Science Foundation of China (81771012 to Z.L. and 81770995 to L.S.) and by a Faculty Research Award from Boehringer Ingelheim International (DE811138149 to Z.L.).

Data availability

All of the mapped data are available from the Sequence Read Archive (SRA) under Accession Number SRP150150.

Supplementary information

Supplementary information available online at
http://dev.biologists.org/lookup/doi/10.1242/dev.168906.supplemental

References

Abe, T., Kakehata, S., Kitani, R., Maruya, S., Navaratnam, D., Santos-Sacchi, J. and Shinkawa, H. (2007). Developmental expression of the outer hair cell motor prestin in the mouse. *J. Membr. Biol.* **215**, 49-56.

Bae, S., Park, J. and Kim, J.-S. (2014). Cas-OFFinder: a fast and versatile algorithm that searches for potential off-target sites of Cas9 RNA-guided endonucleases. *Bioinformatics* **30**, 1473-1475.

Bai, J.-P., Navaratnam, D., Samaranayake, H. and Santos-Sacchi, J. (2006). En block C-terminal charge cluster reversals in prestin (SLC26A5): effects on voltage-dependent electromechanical activity. *Neurosci. Lett.* **404**, 270-275.

Bermingham, N. A., Hassan, B. A., Price, S. D., Vollrath, M. A., Ben-Arie, N., Eatock, R. A., Bellen, H. J., Lysakowski, A. and Zoghbi, H. Y. (1999). Math1: an essential gene for the generation of inner ear hair cells. *Science* **284**, 1837-1841.

Billon, P., Bryant, E. E., Joseph, S. A., Nambiar, T. S., Hayward, S. B., Rothstein, R. and Ciccia, A. (2017). CRISPR-mediated base editing enables efficient disruption of eukaryotic genes through induction of STOP codons. *Mol. Cell* **67**, 1068-1079 e1064.

Brownell, W. E., Bader, C. R., Bertrand, D. and de Ribaupierre, Y. (1985). Evoked mechanical responses of isolated cochlear outer hair cells. *Science* **227**, 194-196.

Cong, L., Ran, F. A., Cox, D., Lin, S., Barretto, R., Habib, N., Hsu, P. D., Wu, X., Jiang, W., Marraffini, L. A. et al. (2013). Multiplex genome engineering using CRISPR/Cas systems. *Science* **339**, 819-823.

Gao, X., Tao, Y., Lamas, V., Huang, M., Yeh, W.-H., Pan, B., Hu, Y.-J., Hu, J. H., Thompson, D. B., Shu, Y. et al. (2018). Treatment of autosomal dominant hearing loss by in vivo delivery of genome editing agents. *Nature* **553**, 217-221.

Gubbels, S. P., Woessner, D. W., Mitchell, J. C., Ricci, A. J. and Brigande, J. V. (2008). Functional auditory hair cells produced in the mammalian cochlea by in utero gene transfer. *Nature* **455**, 537-541.

Hart, T., Chandrashekhar, M., Aregger, M., Steinhart, Z., Brown, K. R., MacLeod, G., Mis, M., Zimmermann, M., Fradet-Turcotte, A., Sun, S. et al. (2015). High-resolution CRISPR screens reveal fitness genes and genotype-specific cancer liabilities. *Cell* **163**, 1515-1526.

He, D. Z., Jia, S., Sato, T., Zuo, J., Andrade, L. R., Riordan, G. P. and Kachar, B. (2010). Changes in plasma membrane structure and electromotile properties in prestin deficient outer hair cells. *Cytoskeleton* **67**, 43-55.

Hu, J. H., Miller, S. M., Geurts, M. H., Tang, W., Chen, L., Sun, N., Zeina, C. M., Gao, X., Rees, H. A., Lin, Z. et al. (2018). Evolved Cas9 variants with broad PAM compatibility and high DNA specificity. *Nature* **556**, 57-63.

Kelley, M. W. (2006). Regulation of cell fate in the sensory epithelia of the inner ear. *Nat. Rev. Neurosci.* **7**, 837-849.

Kelly, M. C., Chang, Q., Pan, A., Lin, X. and Chen, P. (2012). Atoh1 directs the formation of sensory mosaics and induces cell proliferation in the postnatal mammalian cochlea in vivo. *J. Neurosci.* **32**, 6699-6710.

Kim, K., Ryu, S.-M., Kim, S.-T., Baek, G., Kim, D., Lim, K., Chung, E., Kim, S. and Kim, J.-S. (2017a). Highly efficient RNA-guided base editing in mouse embryos. *Nat. Biotechnol.* **35**, 435-437.

Kim, Y. B., Komor, A. C., Levy, J. M., Packer, M. S., Zhao, K. T. and Liu, D. R. (2017b). Increasing the genome-targeting scope and precision of base editing with engineered Cas9-cytidine deaminase fusions. *Nat. Biotechnol.* **35**, 371-376.
Komor, A. C., Kim, Y. B., Packer, M. S., Zuris, J. A. and Liu, D. R. (2016). Programmable editing of a target base in genomic DNA without double-stranded DNA cleavage. *Nature* **533**, 420-424.
Kuscu, C., Parlak, M., Tufan, T., Yang, J., Szlachta, K., Wei, X., Mammadov, R. and Adli, M. (2017). CRISPR-STOP: gene silencing through base-editing-induced nonsense mutations. *Nat. Methods* **14**, 710-712.
Li, C., Shu, Y., Wang, G., Zhang, H., Lu, Y., Li, X., Li, G., Song, L. and Liu, Z. (2018). Characterizing a novel vGlut3-P2A-iCreER knockin mouse strain in cochlea. *Hear. Res.* **364**, 12-24.
Liberman, M. C., Gao, J., He, D. Z. Z., Wu, X., Jia, S. and Zuo, J. (2002). Prestin is required for electromotility of the outer hair cell and for the cochlear amplifier. *Nature* **419**, 300-304.
Liu, X. Z., Ouyang, X. M., Xia, X. J., Zheng, J., Pandya, A., Li, F., Du, L. L., Welch, K. O., Petit, C., Smith, R. J. et al. (2003). Prestin, a cochlear motor protein, is defective in non-syndromic hearing loss. *Hum. Mol. Genet.* **12**, 1155-1162.
Liu, Z., Owen, T., Zhang, L. and Zuo, J. (2010). Dynamic expression pattern of Sonic hedgehog in developing cochlear spiral ganglion neurons. *Dev. Dyn.* **239**, 1674-1683.
Liu, Z., Dearman, J. A., Cox, B. C., Walters, B. J., Zhang, L., Ayrault, O., Zindy, F., Gan, L., Roussel, M. F. and Zuo, J. (2012). Age-dependent in vivo conversion of mouse cochlear pillar and Deiters' cells to immature hair cells by Atoh1 ectopic expression. *J. Neurosci.* **32**, 6600-6610.
Liu, Z., Yang, C.-P., Sugino, K., Fu, C.-C., Liu, L.-Y., Yao, X., Lee, L. P. and Lee, T. (2015). Opposing intrinsic temporal gradients guide neural stem cell production of varied neuronal fates. *Science* **350**, 317-320.
Moser, T. and Beutner, D. (2000). Kinetics of exocytosis and endocytosis at the cochlear inner hair cell afferent synapse of the mouse. *Proc. Natl. Acad. Sci. USA* **97**, 883-888.
Navarrete, E. G. and Santos-Sacchi, J. (2006). On the effect of prestin on the electrical breakdown of cell membranes. *Biophys. J.* **90**, 967-974.
Pangršič, T., Lasarow, L., Reuter, K., Takago, H., Schwander, M., Riedel, D., Frank, T., Tarantino, L. M., Bailey, J. S., Strenzke, N. et al. (2010). Hearing requires otoferlin-dependent efficient replenishment of synaptic vesicles in hair cells. *Nat. Neurosci.* **13**, 869-876.
Rees, H. A., Komor, A. C., Yeh, W.-H., Caetano-Lopes, J., Warman, M., Edge, A. S. B. and Liu, D. R. (2017). Improving the DNA specificity and applicability of base editing through protein engineering and protein delivery. *Nat. Commun.* **8**, 15790.
Roux, I., Safieddine, S., Nouvian, R., Grati, M., Simmler, M.-C., Bahloul, A., Perfettini, I., Le Gall, M., Rostaing, P., Hamard, G. et al. (2006). Otoferlin, defective in a human deafness form, is essential for exocytosis at the auditory ribbon synapse. *Cell* **127**, 277-289.
Ruel, J., Emery, S., Nouvian, R., Bersot, T., Amilhon, B., Van Rybroek, J. M., Rebillard, G., Lenoir, M., Eybalin, M., Delprat, B. et al. (2008). Impairment of SLC17A8 encoding vesicular glutamate transporter-3, VGLUT3, underlies nonsyndromic deafness DFNA25 and inner hair cell dysfunction in null mice. *Am. J. Hum. Genet.* **83**, 278-292.
Ryu, S. M., Koo, T., Kim, K., Lim, K., Baek, G., Kim, S. T., Kim, H. S., Kim, D. E., Lee, H., Chung, E. et al. (2018). Adenine base editing in mouse embryos and an adult mouse model of Duchenne muscular dystrophy. *Nat. Biotechnol.* **36**, 536-539.
Santos-Sacchi, J. (1991). Reversible inhibition of voltage-dependent outer hair cell motility and capacitance. *J. Neurosci.* **11**, 3096-3110.
Seal, R. P., Akil, O., Yi, E., Weber, C. M., Grant, L., Yoo, J., Clause, A., Kandler, K., Noebels, J. L., Glowatzki, E. et al. (2008). Sensorineural deafness and seizures in mice lacking vesicular glutamate transporter 3. *Neuron* **57**, 263-275.
Song, L. and Santos-Sacchi, J. (2013). Disparities in voltage-sensor charge and electromotility imply slow chloride-driven state transitions in the solute carrier SLC26a5. *Proc. Natl. Acad. Sci. USA* **110**, 3883-3888.
Vreugde, S., Erven, A., Kros, C. J., Marcotti, W., Fuchs, H., Kurima, K., Wilcox, E. R., Friedman, T. B., Griffith, A. J., Balling, R. et al. (2002). Beethoven, a mouse model for dominant, progressive hearing loss DFNA36. *Nat. Genet.* **30**, 257-258.
Wang, T., Birsoy, K., Hughes, N. W., Krupczak, K. M., Post, Y., Wei, J. J., Lander, E. S. and Sabatini, D. M. (2015). Identification and characterization of essential genes in the human genome. *Science* **350**, 1096-1101.
Wang, L., Li, M.-Y., Qu, C., Miao, W.-Y., Yin, Q., Liao, J., Cao, H.-T., Huang, M., Wang, K., Zuo, E. et al. (2017). CRISPR-Cas9-mediated genome editing in one blastomere of two-cell embryos reveals a novel Tet3 function in regulating neocortical development. *Cell Res.* **27**, 815-829.
Yao, X., Liu, Z., Wang, X., Wang, Y., Nie, Y.-H., Lai, L., Sun, R., Shi, L., Sun, Q. and Yang, H. (2018). Generation of knock-in cynomolgus monkey via CRISPR/Cas9 editing. *Cell Res.* **28**, 379-382.
Yasunaga, S., Grati, M., Cohen-Salmon, M., El-Amraoui, A., Mustapha, M., Salem, N., El-Zir, E., Loiselet, J. and Petit, C. (1999). A mutation in OTOF, encoding otoferlin, a FER-1-like protein, causes DFNB9, a nonsyndromic form of deafness. *Nat. Genet.* **21**, 363-369.
Yeh, W.-H., Chiang, H., Rees, H. A., Edge, A. S. B. and Liu, D. R. (2018). In vivo base editing of post-mitotic sensory cells. *Nat. Commun.* **9**, 2184.
Zhang, Y., Qin, W., Lu, X., Xu, J., Huang, H., Bai, H., Li, S. and Lin, S. (2017). Programmable base editing of zebrafish genome using a modified CRISPR-Cas9 system. *Nat. Commun.* **8**, 118.
Zheng, J. L. and Gao, W.-Q. (2000). Overexpression of Math1 induces robust production of extra hair cells in postnatal rat inner ears. *Nat. Neurosci.* **3**, 580-586.
Zheng, J., Shen, W., He, D. Z. Z., Long, K. B., Madison, L. D. and Dallos, P. (2000). Prestin is the motor protein of cochlear outer hair cells. *Nature* **405**, 149-155.
Zhou, H., Liu, J., Zhou, C., Gao, N., Rao, Z., Li, H., Hu, X., Li, C., Yao, X., Shen, X. et al. (2018). In vivo simultaneous transcriptional activation of multiple genes in the brain using CRISPR-dCas9-activator transgenic mice. *Nat. Neurosci.* **21**, 440-446.
Zuo, E., Cai, Y.-J., Li, K., Wei, Y., Wang, B.-A., Sun, Y., Liu, Z., Liu, J., Hu, X., Wei, W. et al. (2017). One-step generation of complete gene knockout mice and monkeys by CRISPR/Cas9-mediated gene editing with multiple sgRNAs. *Cell Res.* **27**, 933-945.